Available online at www.sciencedirect.com
ScienceDirect
Carbohydrate Research 343 (2008) 2184–2193
Carbohydrate RESEARCH

# Site-specific interactions of copper(II) ions with heparin revealed with complementary (SRCD, NMR, FTIR and EPR) spectroscopic techniques

T. R. Rudd,[a] M. A. Skidmore,[a] S. E. Guimond,[a] M. Guerrini,[b] C. Cosentino,[b] R. Edge,[c] A. Brown,[d] D. T. Clarke,[d] G. Torri,[b] J. E. Turnbull,[a] R. J. Nichols,[e] D. G. Fernig[a] and E. A. Yates[a,*]

[a]*School of Biological Sciences, University of Liverpool, Liverpool L69 7ZB, UK*
[b]*Institute of Chemical and Biochemical Research 'G Ronzoni', Via G Colombo 81, I-20133 Milano, Italy*
[c]*School of Chemistry, University of Manchester, Oxford Road, Manchester M13 9PL, UK*
[d]*STFC Daresbury Laboratory, Warrington, Cheshire WA4 4AD, UK*
[e]*Department of Chemistry, University of Liverpool, Liverpool L69 7ZD, UK*

Received 20 September 2007; received in revised form 27 November 2007; accepted 17 December 2007
Available online 28 December 2007

Presented at Eurocarb 14th Lübeck, Germany, September 2007

**Abstract**—The interactions between Cu(II) ions and heparin were investigated using several complementary spectroscopic techniques. NMR indicated an initial binding phase involving specific coordination to four points in the structure that recur in slightly different environments throughout the heparin chain; the carboxylic acid group and the ring oxygen of iduronate-2-*O*-sulfate, the glycosidic oxygen between this residue and the adjacent (towards the reducing end) glucosamine and the 6-*O*-sulfate group. In contrast, the later binding phase showed little structural specificity. One- and two-dimensional correlated FTIR revealed that complex out of phase (asynchronous) conformational changes also occurred during the titration of Cu(II) ions into heparin, involving the C=O and N–H stretches. EPR demonstrated that the environments of the Cu(II) ions in the initial binding phase were tetragonal (with slightly varied geometry), while the later non-specific phases exhibited conventional coordination. Visible spectroscopy confirmed a shift of the absorbance maximum. Titration of Cu(II) ions into a solution of heparin indicated (both by analysis of FTIR and EPR spectra) that the initial binding phase was complete by 15–20 Cu(II) ions per chain; thereafter the ions bound in the non-specific mode. Hetero-correlation spectroscopy (FTIR–CD) improved resolution and assisted assignment of the broad CD features from the FTIR spectra and indicated both in-phase and more complex out of phase (synchronous and asynchronous, respectively) changes in interactions within the heparin molecule during the titration of Cu(II) ions.


*Keywords:* Heparin; Copper; SRCD; NMR; FTIR; EPR; Two-dimensional-correlation spectroscopy

*Abbreviations*: SRCD, synchrotron radiation circular dichroism; FGF, fibroblast growth factor; FGFR, fibroblast growth factor receptor; PCA, prinicipal component analysis; GAG, glycosaminoglycan; HS, heparan sulfate; HSPG, heparan sulfate proteoglycan; A refers to amino sugar (glucosamine) residues and I to iduronate (IdoA) residues; A-*N* refers to the Nth hydrogen or carbon atom of the glucosamine residue and I-*N* to the Nth hydrogen or carbon atom of the iduronate residue. IdoA2S refers to iduronate-2-*O*-sulfate; GlcNS, GlcNS6S and GlcNAc to glucosamine *N*-sulfate, glucosamine *N*-sulfate, 6-*O*-sulfate and *N*-acetyl glucosamine, respectively

* Corresponding author. Tel.: +44 (0)151 795 4429; e-mail: eayates@liv.ac.uk

0008-6215/$ - see front matter © 2008 Elsevier Ltd. All rights reserved.
doi:10.1016/j.carres.2007.12.019

## 1. Introduction

The linear, sulfated polysaccharide heparin has long been used as an anticoagulant as a result of its interaction with the serum protease antithrombin, which increases the affinity of antithrombin for factor $X_a$ by several orders of magnitude. Heparin also exhibits many other activities in a wide range of biological assays, which include the ability to support formation of active signalling complexes with fibroblast growth factors and their receptors (FGF/FGFR),[1,2] an ability to inhibit a range of other proteases including BACE-1, the Alzheimer's β-secretase,[3] renin, cathepsin-D and many others. These activities presumably arise from the structural similarities between the glycosaminoglycans (GAG) heparin and heparan sulfate (HS). HS is the naturally occurring cell-surface and extracellular matrix expressed polysaccharide component of heparan sulfate proteoglycans (HSPGs), which modulate these activities in vivo. Both heparin and HS are based on a linear backbone comprising a basic disaccharide repeating unit, composed of (1→4)-linked uronic acid and α-D-glucosamine. In the case of heparan sulfate, the uronic acid is predominantly β-D-GlcA while in heparin it is the C-5 epimer α-L-IdoA. The uronic acid residues can be 2-O-sulfated or unsubstituted and glucosamine can be 6-O-sulfated, N-acetylated, unsubstituted or N-sulfated. More rarely, glucosamine can be found 3-O-sulfated and this residue is crucial to the binding of antithrombin,[4] which involves a specific pentasaccharide sequence.

The polyanionic nature of heparin necessitates interaction with counter ions and this has been the subject of many studies using a range of physico-chemical techniques. These have included viscosity, polarimetry, circular dichroism (CD), infrared (IR) spectroscopy, nuclear magnetic resonance spectroscopy (NMR) and others.[5–16] Recently, we have shown by a combination of synchrotron radiation circular dichroism (SRCD) and NMR spectroscopy that most combinations of heparin derivatives and the cations Na, K, Mg, Ca, Fe(III), Mn(II) and Cu(II) interact in structurally distinct ways.[17] Conversion of certain heparin derivatives to particular cation forms, particularly Cu(II) and K, also resulted in drastically altered signalling characteristics in a cell-based assay of FGF-2/FGFR1c signalling[17] demonstrating that in structure–activity terms, the sequence or substitution pattern alone cannot determine activity; the associated cations also need to be considered.

Circular dichroism (CD, and its synchrotron radiation development SRCD) spectra are sensitive to the chiral environment of chromophores in the C=O bonds of carboxylic acids and *N*-acetyl groups (arising from $n\rightarrow\pi^*$ and $\pi\rightarrow\pi^*$ transitions) in the carboxylic acid and *N*-acetyl groups of heparin derivatives.[18] The unique nature of SRCD spectra of heparin complexes with cations[17] implies that many cation–polysaccharide interactions are structurally distinct at the level detected by SRCD. Analysis of the spectra through their principal components revealed that Cu(II) derivatives consistently exhibited the most distinct spectra. There has been considerable work done on the interaction of cations with heparin and recent examples include the study of Na, K, Mg and Ca ion binding to heparin-based oligosaccharides involving NMR and molecular modelling. Calcium was found to bind specifically between IdoA and GlcN residues, while Na, K and Mg were less specific. Furthermore, Ca binding induced a change in the equilibrium of conformers in IdoA towards $^1C_4$ and involved interactions between the carboxylic acid group and *O*-sulfate of the uronic acid and the *N*-sulfate group of glucosamine. It also involved the ring and glycosidic oxygens and water resulting in a square bipyramidal coordination geometry.[5,6] Study of the interactions of heparin with Cu(II) ions is also long established but, despite a number of distinct approaches being applied,[7–17] the details remain ill-defined. Using a combination of CD and viscosity measurements, it was established that Cu–heparin behaved differently to other cation forms of heparin.[7] The carboxylic acid and sulfate groups were both proposed as being involved in the interaction with Cu(II)[7,15] and a range of association constants have been calculated.[19] The stoichiometry of the interaction has also been studied, the suggestion of multiple binding sites being made early on[19] and estimates of binding stoichiometry approaching one Cu(II) ion per disaccharide unit 4-L-IdoA2S-α-4-D-GlcNS,6S-α-1- have been proposed.[16] FTIR techniques have also established that the carboxylic acid group is directly involved in the interaction with Cu(II) and the interaction is not thermodynamically reversible in a simple equilibrium[8,9] suggesting the involvement of several modes of binding. However, a more precise understanding of these interactions has remained elusive.

There is extensive literature concerning the involvement of Cu(II) ions in cellular processes, particularly angiogenesis[20,21] and some of these activities are also known to require the interaction of heparin/heparan sulfate polysaccharides with growth factors. It is also well-documented that the level of Cu(II) ions in serum increases dramatically during pregnancy and tumourigenesis.[22] Recently, Cu(II) ions have been found to modify signalling activities in FGF/FGFR cell signalling assays, converting a polysaccharide incapable of supporting signalling through FGF-2/FGFR1c into one capable of signalling; an effect that was not caused by free Cu(II) ions.[17] The study of the interactions between carbohydrates and cations is important from the point of view of toxicity and will contribute towards a better understanding of the involvement of ions in synthetic and degradative processes.[23]

As part of our on-going investigations into the structural basis of the interactions of ions with heparin derivatives, we examined the interaction of Cu(II) with intact

heparin employing a number of complementary spectroscopic techniques. Cu(II) ions are relatively unusual among physiologically relevant cations in exhibiting paramagnetic behaviour, a property that arises from possession of an unpaired electron in the outer electron shell ($d^9$) and this offers a number of experimental opportunities utilising magnetic resonance techniques. In the case of NMR, the location of coordinated Cu(II) ions can be inferred from the line broadening and reduced signal intensity of nuclei in the vicinity, while EPR can detect changes in the environment of the copper ion itself. These two techniques therefore offer highly complementary information. The paramagnetic property of Cu(II) ions is, however, something of a drawback regarding the use of NMR to obtain conformational and dynamic information because the accurate measurement and analysis of coupling constants and relaxation times is severely compromised by their presence.

Aqueous salts of Cu(II) ions have long been described as octahedrally coordinated, but this has recently been challenged, and an alternative fivefold coordination proposed.[24] Cu(II) complexes of organic molecules, on the other hand, are known to adopt alternative coordination arrangements, particularly tetragonal[25] and these exhibit distinct spectral properties in the visible range resulting from Jahn–Teller distortion.[26]

FTIR spectroscopy is useful for detecting C=O stretching vibrations in uronate residues, some of which (IdoA2S and IdoA) are known to undergo conformational changes[27,28] potentially providing additional and complementary information to magnetic resonance techniques. Changes in the intensity and position of the carboxylate C=O stretching frequency (1620–1610 $cm^{-1}$) as Cu(II) ions are added to a sample of heparin can be detected and correlated (in two IR frequency domains) on the basis of a generalised approach for two-dimensional-correlation spectroscopy (2D-COS) proposed by Noda,[29,30] in terms of those changes which occur simultaneously (in-phase) during the addition of copper (the perturbation), termed synchronous changes, and also in terms of those occurring in an unsynchronised manner (out of phase), termed asynchronous changes.

Employing a combination of these methods, it has been possible to define the nature of Cu(II) binding to unmodified heparin, locate the specific sites and the extent of its initial interactions and detect complex conformational changes that occur during binding.

## 2. Results and discussion

### 2.1. Cu(II) ions interact with heparin in a way that is distinct from other common cations

The SRCD spectra of heparin in a range of cationic forms (Na, K, Mg, Ca and Cu(II)) have been recorded (Fig. 1). The interactions gave rise to different spectra in each case (Fig. 1A and analysis by PCA, Fig. 1B), with the Cu(II) form being most distinct. In this experiment, SRCD was sensitive to the chiral environment of the chromophore present in the carboxylic acid of the uronic acid. For heparin, the negative band at 210 nm has been assigned to the $n\rightarrow\pi^*$ transition of the carboxylate group[18] and the higher energy positive band at 190 nm has been assigned to multiple oxygen chromophores (e.g., glycosidic linkage, ring and hydroxyl groups,[31] with contributions from the *N*-sulfate group[32]). These results suggested that the interaction between Cu(II) and heparin may be distinct from the other common cations. The nature of this interaction was explored further through one- and two-dimensional NMR, FTIR and EPR techniques. Two noticeable features of the spectrum for Cu(II) ion-exchanged heparin compared to the other common cations (Fig. 1A) are that the minimum at 190 nm diminishes, with the spectrum flattening out after the maximum and the position of the maximum is intermediate between the mono- and divalent cation groups at 188 nm (Fig. 1A), but the spectrum is not a composite of those formed with the other cations. The evolution of the Cu(II):heparin spectrum can be seen with a copper concentration gradient (Fig. 1C); with increasing Cu(II) ion concentration, the maximum moves from 192 to 188 nm, with the amplitude of the peak increasing (Fig. 1C). The maximum disappears at ca. 20 ions per heparin chain. There is an isodichroic point (~219 nm) for the samples with lower equivalents of Cu(II) ions per heparin chain, suggesting an equilibrium of 2 forms, but after this point the spectra move away from the convergent point suggesting more complex processes. The spectra between 200 and 260 nm clearly illustrate that the interaction of heparin with Cu(II) has at least two distinct steps, occurring between 0–10 and 20–60 Cu(II) ions per heparin chain [see Supplementary data for separate plots of the maximum at 190 nm and minimum at 210 nm and the position of the maximum at 190 nm with Cu concentration].

The 2D-correlated[30] synchronous treatment of the SRCD spectra (Fig. 1D) provides a clear illustration of the changes occurring simultaneously between the two IR dimensions as Cu(II) ions are taken up by heparin, with all the auto peaks (183, 209 and 234 nm) having common cross peaks. Changes in the synchronous spectrum correspond to in-phase changes in spectra; in this case, the shift to lower wavelengths of the maximum at 190 nm and the simultaneous shallowing and disappearance of the peak at ~210 nm to leave a slightly curved, featureless region. The asynchronous correlation spectrum exhibits correlations between 209, 197 and 186 nm, and represents those features which change in an unsynchronised or sequential manner (see Supplementary data). Other complex changes around 227 nm correlate with that at 207 nm. Broad features between

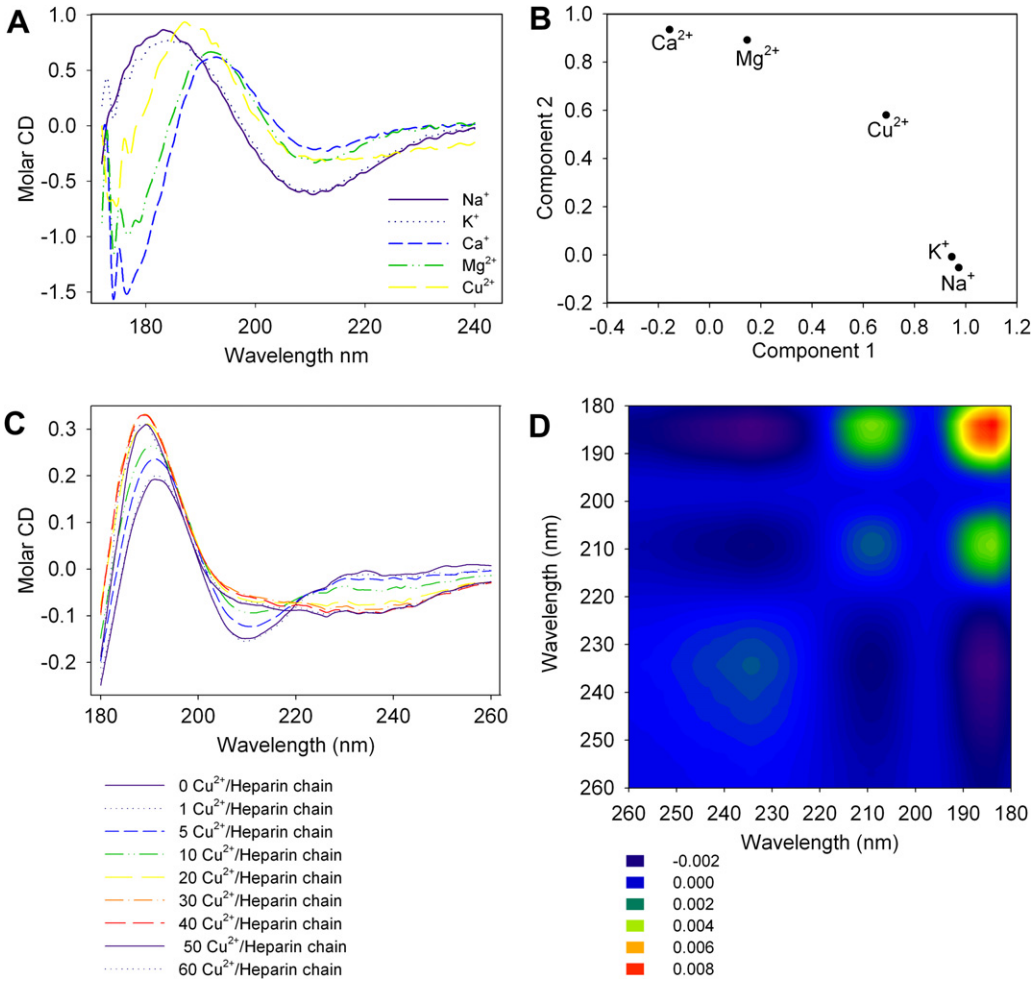


**Figure 1.** (A) SRCD spectra of heparin converted to the Cu(II) form and a range of common cation forms; Na, K, Mg, Ca. (B) Principal component analysis (PCA) of the SRCD spectra, illustrating the distinct nature of the Cu(II) form. (C) Cu(II) concentration gradient with 10 mg/mL heparin with increasing equivalents (from 0 to 60 cations per heparin chain). (D) Synchronous 2D CD spectrum of the Cu(II) gradient. In-phase changes (changes which correlate in-phase during the addition of Cu(II) ions) are exhibited as off-diagonal cross-peaks.

220 and 245 nm correlate with higher energy signals below 200 nm.

### 2.2. The initial site of interaction of Cu(II) ions with heparin is specific

The effect of adding paramagnetic Cu(II) ions is to alter the relaxation rates of nuclei involved in binding, resulting in line broadening and signal diminution in NMR spectra. This process can be followed by observing $^{1}H$ spectral projections of 2D NMR spectra (HSQC previously fully assigned[33]) in which both $^{1}H$ and $^{13}C$ dimensions are shown to assist peak identification (Fig. 2A and B). The initial sites of interaction of Cu(II) are with the iduronic acid 2-*O*-sulfate residues, causing a reduction in signal intensity of the I-5 signal ($^{1}H$ and $^{13}C$ chemical shifts 4.9 ppm, 72 ppm) (Fig. 2A). As more Cu(II) is added (Fig. 2B), the signals from I-1 of IdoA2S ($^{1}H$ and $^{13}C$ chemical shifts at 5.3 ppm, 102 ppm) diminish, but not those of position-1 from either IdoA or GlcA (at ca. 104 and 105 ppm, respectively, in the $^{13}C$ spectra). The A-4, A-5 and A-6 signals of glucosamines were also affected. This implies that the Cu(II) ion is coordinating the carboxylic acids and ring oxygens of the IdoA2S residues, the glycosidic oxygen (between the IdoA2S residue and glucosamine-6-*O*-sulfate, *N*-sulfate) and the 6-*O*-sulfate groups. Thus, the divalent requirement of each Cu(II) cation is satisfied and four ligands are provided by specific positions, which are repeated along the heparin polysaccharide chain. The interaction is specific to the sequence (IdoA2S–Glc[NS/NAc]6S) and does not bind to sequences containing either IdoA or GlcA in this initial phase, the signals arising from IdoA and GlcA being unaffected in this initial binding phase. Further additions of Cu(II) ions cause a general broadening of the lines in the spectrum and reduction in signal intensity with little apparent selectivity. This indicates a second phase in which more general binding to the remaining charged groups of heparin occurs.

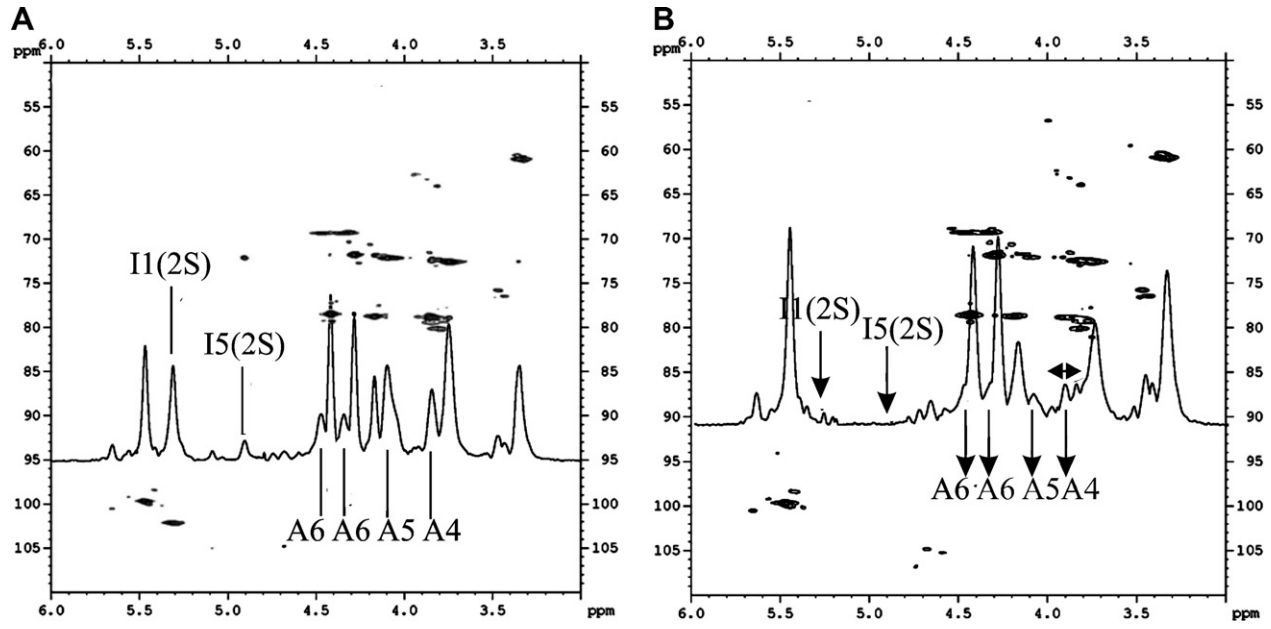


**Figure 2.** (A) HSQC spectrum of heparin in the presence of trace amounts of Cu(II) ions showing $^{1}H$ and $^{13}C$ correlation and a projection of the $^{1}H$ spectrum exhibiting line broadening and signal diminution at specific positions (indicated). (B) HSQC spectrum of heparin with ca. 20 cations per chain equivalents of Cu(II) ions showing further signal diminution at specific positions.

### 2.3. FTIR spectra of the titration of Cu(II) ions into heparin allows the initial phase of binding to be differentiated from later, general binding and permits quantification of Cu(II) binding

1-D transmission FTIR spectra of heparin titrated with Cu(II) ions are shown in Figure 3A and an expansion of the C=O stretching region is shown in Figure 3B. A plot of the shift in the position of the C=O stretch (1610–1620 $cm^{-1}$) as a function of the number of Cu(II) equivalents added per heparin chain (Supplementary data) revealed a two-phase binding process, the initial phase being complete by ca. 20 equiv per heparin chain and the second phase by around 40 ppm. 2D plots of the C=O stretch spectral position revealed those changes which correlated simultaneously (in-phase) during the addition of Cu(II) ions; synchronous correlations (Fig. 3C), and those which correlated out of phase; asynchronous correlations (Fig. 3D), which probably arose from more complex changes in conformation. The synchronous spectrum (Fig. 3C) has four auto peaks at 1622, 1598, 1460 and 1419 $cm^{-1}$. The first two peaks at 1622 and 1598 $cm^{-1}$ have two corresponding negative cross peaks, due to the shift in the position of the carboxylic acid band. Both of these auto peaks at 1622 and 1598 $cm^{-1}$ form correlation squares with the large and predominant auto peak at 1461 $cm^{-1}$, with cross peaks at 1468, 1419 and 1338 $cm^{-1}$, respectively.

These cross peaks confirm the interconnectivity of the bands due to the carboxylate group and the multiple bands that are present centred around 1462 $cm^{-1}$, some of which arise from N–H stretching. This suggests a change in the interaction between the carboxylic acid and nitrogen of glucosamine and/or a conformational change, which alters the interactions in which these two groups are participating.

The asynchronous spectrum reveals a wealth of correlations most notably between 1620, 1598 and 1460 $cm^{-1}$, and a broad feature between 1280 and 1380 $cm^{-1}$ (the latter being the sulfate stretching region).

### 2.4. Features in the FTIR and SRCD spectra can be resolved through FTIR–CD hetero-correlation analysis

The correlation of two spectra from different spectral ranges (hetero-correlation) offers a number of advantages. One of these is improved resolution, arising from the spreading of one spectral dimension into a second. In favourable cases, there will be sufficient differentiation to be able to distinguish and hence assign previously superimposed signals. An example of this is shown in Figure 4, in which the FTIR and SRCD spectra of heparin titrated with Cu(II) ions are shown with both synchronous (Fig. 4A) and asynchronous (Fig. 4B) analyses. The synchronous correlation (Fig. 4A) indicated those changes which arose from changes in the two spectra that correlated in-phase during the perturbation (i.e., addition of Cu(II) to the system). There was a correlation between the C=O stretch of the carboxylate (1610 $cm^{-1}$) and two features in the SRCD spectrum at 215 and 190 nm and these were also correlated with signals that included the N–H stretch at 1415 $cm^{-1}$.

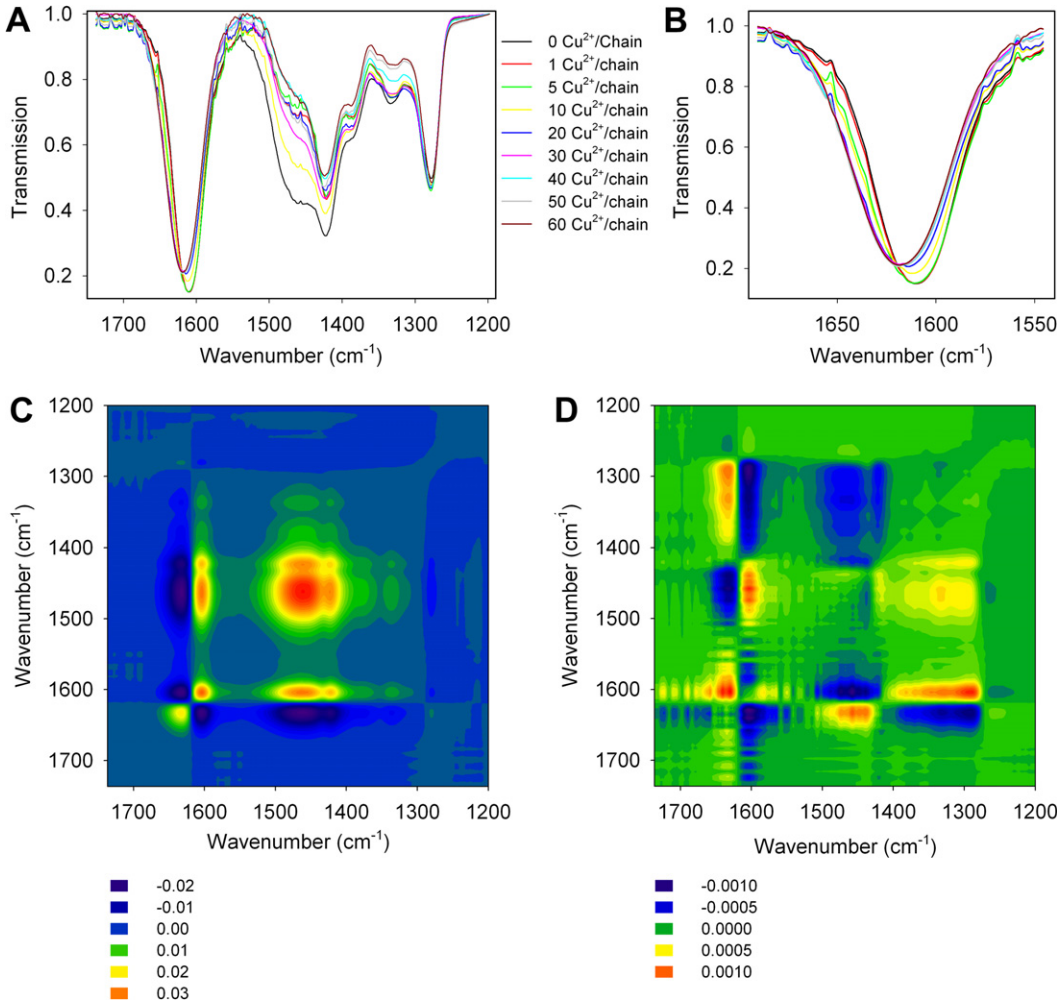


**Figure 3.** (A) One-dimensional FTIR transmission spectra of heparin titrated with Cu(II) ions (0–60 cations per chain). (B) Expansion of the spectra in the C=O stretch region (1610–1620 $cm^{-1}$), which arises predominantly from the carboxylate group. (C) Synchronous 2D correlation FTIR spectrum of heparin titrated with Cu(II) ions. (D) Asynchronous 2D correlation FTIR spectrum of heparin titrated with Cu(II) ions.

It seems more likely that features in synchronous hetero-correlated spectra are related to the same structural feature despite (in this case) one dimension being transmission FTIR and the other circular dichroism (CD) because they report processes that alter together during a perturbation and their respective spectral positions suggest that they may arise from the same chemical group. Asynchronous hetero-correlated spectra, on the other hand, are likely to be dominated by features with more complex relationships relating to sequential conformational changes.

Analysis of the asynchronous correlation (Fig. 4) reveals that the C=O stretch arising from the carboxylic acid at 1610 $cm^{-1}$ is correlated with two broad features in the SRCD spectrum; one (positive) between 232 and 242 nm, associated with the carboxylic acid group in the SRCD spectrum[18,31] and higher (negative) energy transitions centred at 183 and 188 nm. Another C=O stretch, arising from the acetyl group in heparin at 1640 $cm^{-1}$ correlates with higher energy transitions centred at 192 nm. The N–H stretch at 1430 $cm^{-1}$ also correlates with a CD feature at 235 nm. All of these features in the FTIR spectrum also correlate with narrow, high energy bands at 183 and 185 nm. Congested features, for example, in the C=O stretching region between 1600 and 1630 $cm^{-1}$ are thereby resolved into separate bands indicating different behaviour of C=O groups in distinct environments during the addition of Cu(II) ions. The signal at 1630 $cm^{-1}$ correlates with the CD band at 195 nm, that at 1610 $cm^{-1}$ with those at 236, 210 and 183 nm, while that at 1598 $cm^{-1}$ with those at 186 and 183 nm. The complex bands, which include N–H stretching between 1400 and 1500 $cm^{-1}$, correlate with CD bands at 210, 197, 186 and 183 nm.

### 2.5. The coordination geometry of the Cu(II) ion is distinct for the two binding phases

The environment of the paramagnetic Cu(II) ion can also be investigated by electron paramagnetic resonance

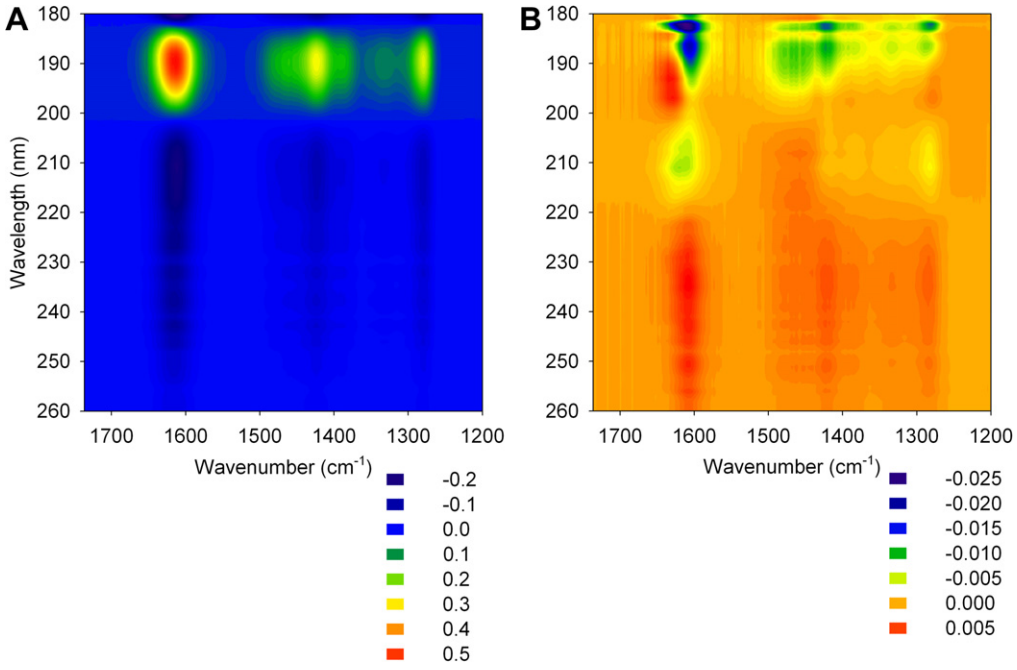


**Figure 4.** (A) Synchronous correlation of FTIR spectrum and SRCD spectrum of Cu(II) titration of heparin. (B) Asynchronous correlation of FTIR spectrum and SRCD spectrum of Cu(II) titration of heparin.

(EPR) spectroscopy. Hydrated Cu(II) ions present a broad, symmetrical EPR feature (Fig. 5A). It has long been held that in free aqueous solution, at room temperature, hydrated Cu(II) ions are coordinated in a symmetrical octahedral arrangement but this has recently been challenged.[24] In the case of coordination to heparin at a low ratio of Cu(II) ions per heparin chain (Fig. 5B), different features arise, in which the four *z*-components (*g*-values of which are 2.24, 2.32, 2.40 and 2.49) are clearly separated from the *x*- and *y*-components, the latter pair of which are equivalent and appear as one feature.[34] This is consistent with the Cu(II) ions being coordinated in near equivalent tetragonal arrangements throughout the heparin chain and this appears to be the sole mode of binding until a ratio of Cu(II) ions per heparin chain in excess of ca. 15–20 is obtained (Fig. 5C and D). At higher ratios, a broad feature is superimposed progressively onto the spectra and finally dominates (Fig. 5C). This is consistent with the later Cu(II) ions being coordinated in a conventional arrangement and may also include signals from excess Cu(II) ions that are not coordinated to heparin. The evolution of the bands can also be clearly seen through the synchronous and asynchronous two-dimensional plot of the EPR spectra (see Supplementary data).

The results of NMR spectroscopy indicate that a specific interaction occurs when Cu(II) ions are initially titrated into heparin, involving coordination of the carboxylic acids and ring oxygens of the IdoA2S residues (but not IdoA and GlcA) the glycosidic oxygens between IdoA2S and GlcNS6S residues and the 6-*O*-sulfate group of the adjacent GlcNS residues. This arrangement allows the divalent charge on the ion to be satisfied by charged groups on a single chain and the EPR spectra of Cu(II) complexes in water at room temperature resemble those observed in powder spectra, implying relatively low mobility of the Cu(II) complexed heparin polysaccharide in solution.

The conventionally coordinated Cu(II) ion in aqueous solution presents a symmetrical EPR spectrum[34] in contrast to that observed when Cu(II) ions initially bind heparin. The resulting EPR spectra of heparin suggest a fourfold coordination, in which to a first level of analysis, the four points of coordination are planar and symmetrical, the other(s), if present, presumably being more distant water molecules. This distorted arrangement is well-known for Cu(II) ions complexed with organic materials and is predicted to give rise to small changes in transitions between energy levels, known as a Jahn–Teller effect.[26] A small change in the visible absorbance spectrum was observed when 10 ions per chain were examined consistent with this effect. The sample became visibly 'bluer' than the Cu(II) ion alone control and a consistent shift in the absorption maximum [190 nm] to lower wavelengths (20–25 nm) and increased absorbance for several independent preparations compared to the equivalent free Cu(II) control solution were observed. Initial binding of Cu(II) ions to these repeated, near-identical positions resulted in a number of ions bound along the heparin chain in positions of near equivalence, supported by the relatively well-resolved EPR spectra at low ratios of copper to heparin. There is some evidence from the EPR spectra for the existence of several similar tetragonal binding arrangements

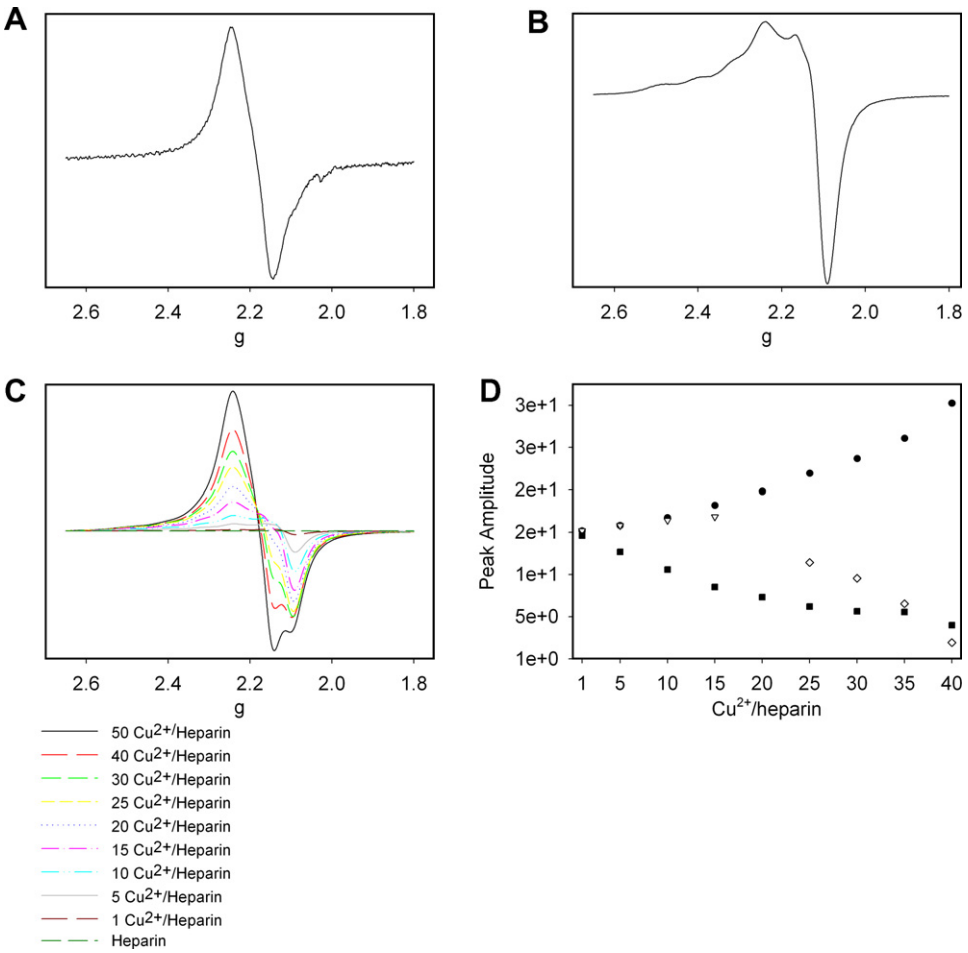


**Figure 5.** (A) Cu(II) ions in dilute aqueous solution in which the Cu(II) ion is conventionally coordinated (X-band, 298 K) exhibit equivalent *x*-, *y*- and *z*-components. (B) Cu(II) ions coordinated to heparin in the ratio 10:1 (X-band, 298 K) showing distinct *z*-components and equivalent *x*- and *y*-components consistent with approximately equivalent, tetragonal coordination geometries in the initial binding phase. (C) Titration of Cu(II) ions into heparin as a ratio of ions per heparin chain (X-band, 298 K). (D) Plot of the evolution of major peaks present in (B) (the major features at 2.24, 2.16, 2.14 and 2.09 g).

during this initial phase and these may correspond to the areas of sequence heterogeneity, or result from conformational changes in adjacent residues as $Cu^{2+}$ ions progressively bind. As more copper is added, however, a general, less specific binding occurs, finally dominating the spectra. The initial spontaneous binding of Cu(II) ions to specific features of the intact heparin sequence must be thermodynamically favourable. There are several possible contributing factors; formation of favourable, multiple bonds between Cu and the four coordination points, a net gain in solvent entropy between hydrated, octahedrally coordinated copper ions and hydrated Na ions. These favourable factors must more than compensate for the increased rigidity of the Cu-coordinated polysaccharide, which, perhaps, is further assisted by increased entropy in the bulk water surrounding the polysaccharide.

The specific coordination of the points in the heparin structure, preferentially in the initial binding phase, reflects their appropriate spatial arrangement. They must be co-planar and situated approximately at the corners of a rectangle in order that they can form a tetragonal binding arrangement with the Cu(II) ions (Fig. 6).

The application of correlation spectroscopy methods both between spectra of the same spectral range (homo-correlations; e.g., either FTIR–FTIR or CD–CD) and between different spectral regions (hetero-correlations; in this case between FTIR and CD spectral regions) has been informative and, besides improving spectral resolution and assignment, was very useful to distinguish between those correlations which changed simultaneously during the addition of Cu(II) and those which involved more complex sequential changes in both spectral regions. Among the latter, the correlation between a C=O stretch from *N*-acetyl at 1630 $cm^{-1}$ and electronic transitions around 190–196 nm is interesting.

Complex conformational changes may include, for example, the making or breaking of a hydrogen bond involving this residue and/or indirect conformational consequences of Cu(II) binding, indicating those spec-

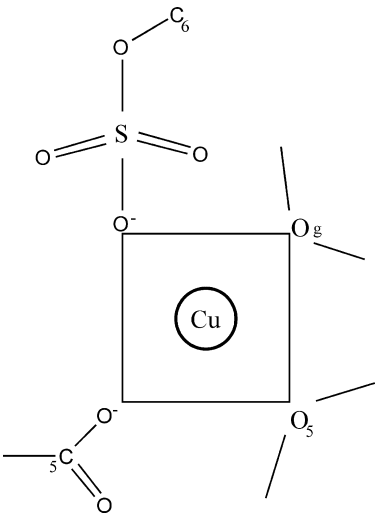


**Figure 6.** Schematic of the proposed generalised tetragonal coordination of Cu(II) ions to the four groups of the predominant heparin disaccharide repeat; 4-L-IdoA2S-α-4-D-GlcNS,6S-α-1-.

tral features (in either SRCD, FTIR or both) that could be used to follow it. It also highlights a potential route for the selective excitation of these interactions, which could be monitored through other spectral features via pump-probe experiments.

Analysis of FTIR and EPR spectra of copper(II) ions titrated into heparin both indicate that the initial phase of coordination, as shown by NMR spectroscopy results, was relatively specific involving tetrahedral coordination. This appears to proceed until between 10 and 20 ions have coordinated each heparin chain, which implies a stoichiometry close to one cation per disaccharide repeat of 4-L-IdoA2S-α-4-D-GlcNS,6S-α-1- as proposed by Crescenzi et al.[16] After this, a general interaction with little evidence of structural specificity is indicated in which ion coordination is consistent with conventional coordination geometry in aqueous solution. 2D FTIR spectral analysis shows that structural changes occur both in-phase during the addition of Cu(II) ions (via synchronous spectra) and out of phase (via asynchronous spectra). The latter demonstrates that complex sequential conformational changes occur within the heparin molecule following the binding of Cu(II) ions and these include modified C=O and N–H stretching and result in complex conformational change.

## 3. Experimental

### 3.1. Reagents

Porcine mucosal heparin (lot PH-42800) was obtained from Celsus Laboratories, Cincinnati, OH, USA. Copper(II) chloride and deuterium oxide were obtained from Sigma–Aldrich, Gillingham, Dorset, UK.

### 3.2. Synchrotron radiation circular dichroism spectroscopy

SRCD spectra were recorded on the purpose-built CD-12 beamline at Daresbury Laboratory (Warrington, UK), between 260 and 180 nm in $D_2O$, using a 0.01 mm quartz cell with 1 nm resolution. Results are expressed as molar ellipticity ($mol^{-1}\,cm^{-1}$) with reference to a solution of (+)-10-camphorsulfonic acid (CSA) at 10 mg $mL^{-1}$ in water. Principal component analysis was performed using SPSS (SPSS Ltd UK, Woking, Surrey, UK).

### 3.3. Nuclear magnetic resonance spectroscopy

NMR spectra were recorded essentially as previously described.[17] Chemical shift values were measured downfield from trimethylsilyl propionate (sodium salt) as standard at 308 K. All proton detected spectra were recorded on a Bruker Avance 600 instrument equipped with cryogenic TXI 5 mm probe. Spectra were assigned using a combination of COSY, TOCSY and HSQC spectra. Copper(II) ions (as the chloride) were added in $D_2O$, calculated as a percentage equivalent of the theoretical charge of heparin based on its composition.[35,36] The 2D experiment matrix size of 2K × 320 was zero filled to 4K × 2K by the application of a squared cosine function before Fourier transformation.

### 3.4. Fourier transform infrared spectroscopy

FTIR spectra were recorded on a Bruker IFS 66v/S spectrometer (Bruker Optics Limited, Coventry, UK), using a MCT liquid nitrogen cooled detector. The spectra were made up of 3000 scans at a resolution of 2 $cm^{-1}$, using an Omnicell sample holder with $CaF_2$ windows (Specac Ltd, Orpington, Kent, UK), the spectrometer being purged with nitrogen gas. The spectra were analysed using OPUS software (Bruker Optics Limited, Coventry, UK) and graphed in Sigmaplot (Systat Software Inc, Hounslow, UK).

### 3.5. Two-dimensional-correlation spectroscopy

2D Correlation spectra were generated using the Bruker OPUS software (Bruker Optics Limited, Coventry, UK) and the freely available 2Dshige software (http://sci-tech.ksc.kwansei.ac.jp/~ozaki/2D-shige.htm) and graphed in Sigmaplot (Systat Software Inc, Hounslow, UK).

### 3.6. Electron paramagnetic resonance spectroscopy

EPR measurements were recorded on a Bruker Biospin EMX micro spectrometer [X-band 9 GHz] (Bruker BioSpin Limited, Coventry, UK). The spectra were recorded at room temperature (298 K), in deuterium

oxide, for high concentrations only one scan was required, at lower concentrations a spectrum is an average of 10 scans. Analysis was performed using the Bruker WinEPR suite of software (Bruker BioSpin Limited, Coventry, UK).

### 3.7. Visible spectroscopy

Spectra were collected using a Molecular Devices/SpectraMax micro plate reader and the SoftMax Pro software package (Molecular Devices Ltd, Wokingham, Berkshire, UK). Samples were loaded in a 96 well plate, the region 700–1000 nm was scanned at a resolution of 1 nm at room temperature (298 K). The titration of Cu(II) ions ($CuCl_2$ in $H_2O$) into heparin experiments was based on the number of ions per polysaccharide chain, calculated on an average molecular weight of 12 kDa, corresponding to ca. 20 disaccharide repeating units.

## Acknowledgements

The authors acknowledge funding from the BBSRC to EAY (TDI) and JET, DGF and EAY (SCIBS). EPSRC for access to the national EPR service at the University of Manchester and Science and Technology Facilities Council for access to beamline 12.1 (SRCD) at Daresbury Laboratory.

## Supplementary data

Supplementary data associated with this article can be found, in the online version, at doi:10.1016/j.carres.2007.12.019.

## References

1. Gallagher, J. T. *Biochem. Soc. Trans.* **2006**, *34*, 438–441.
2. Ornitz, D. M.; Xu, J.; Colvin, J. S.; McEwen, D. G.; MacArthur, C. A.; Coulier, F.; Gao, G.; Goldfarb, M. *J. Biol. Chem.* **1996**, *271*, 15292–15297.
3. Scholefield, Z.; Yates, E. A.; Wayne, G.; Amour, A.; McDowell, W.; Turnbull, J. E. *J. Cell Biol.* **2003**, *163*, 97–107.
4. Grootenhuis, P. D. J.; Westerduin, P.; Meuleman, D.; Petitou, M.; Vanboeckel, C. A. A. *Nat. Struct. Biol.* **1995**, *2*, 736–739.
5. Chevalier, F.; Angulo, J.; Lucas, R.; Nieto, P. M.; Martin-Lomas, M. *Eur. J. Org. Chem.* **2002**, 2367–2376.
6. Chevalier, F.; Lucas, R.; Angulo, J.; Martin-Lomas, M.; Nieto, P. M. *Carbohydr. Res.* **2004**, *339*, 975–983.
7. Chung, M. C. M.; Ellerton, N. F. *Biopolymers* **1976**, *15*, 1409–1423.
8. Grant, D.; Long, W. F.; Moffat, C. F.; Williamson, F. B. *Biochem. J.* **1992**, *283*, 243–246.
9. Grant, D.; Long, W. F.; Williamson, F. B. *Biochem. J.* **1992**, *285*, 477–480.
10. Herwats, L.; Laszlo, P.; Genard, P. *Nouv. J. Chim.* **1977**, *1*, 173–176.
11. Liu, Z.; Perlin, A. S. *Carbohydr. Res.* **1992**, *236*, 121–133.
12. Mukherjee, D. C.; Park, J. W.; Chakrabarti, B. *Arch. Biochem. Biophys.* **1978**, *191*, 393–399.
13. Panov, V. P.; Ovsepyan, A. M. *Vysokomol. Soedin. A+* **1984**, *26*, 1963–1970.
14. Rej, R. N.; Holme, K. R.; Perlin, A. S. *Carbohydr. Res.* **1990**, *207*, 143–152.
15. Stivala, S. S.; Liberti, P. A. *Arch. Biochem. Biophys.* **1967**, *122*, 40–54.
16. Crescenzi, V.; Airoldi, C.; Dentini, M.; Pietrelli, L.; Rizzo, R. *Macromol. Chem. Phys.* **1981**, *182*, 219–223.
17. Rudd, T. R.; Guimond, S. E.; Skidmore, M. A.; Duchesne, L.; Guerrini, M.; Torri, G.; Cosentino, C.; Brown, A.; Clarke, D. T.; Turnbull, J. E.; Fernig, D. G.; Yates, E. A. *Glycobiology* **2007**, *17*, 983–993.
18. Morris, E. R.; Rees, D. A.; Sanderson, G. R.; Thom, D. *J. Chem. Soc., Perkin Trans. 2* **1975**, 1418–1425.
19. Stivala, S. S.; Yadlowsky, S.; Yuan, L. *Biopolymers* **1973**, *12*, 947–959.
20. Alessandri, G.; Raju, K.; Gullino, P. M. *Microcirc. Endoth. Lym.* **1984**, *1*, 329–346.
21. Alessandri, G.; Raju, K. S.; Gullino, P. M. *Cancer Res.* **1983**, *43*, 1790–1797.
22. Trumbo, P.; Schlicker, S.; Yates, A. A.; Poos, M. *J. Am. Diet Assoc.* **2002**, *102*, 1621–1630.
23. Liu, Z.; Perlin, A. S. *Carbohydr. Res.* **1994**, *255*, 183–191.
24. Pasquarello, A.; Petri, I.; Salmon, P. S.; Parisel, O.; Car, R.; Toth, E.; Powell, D. H.; Fischer, H. E.; Helm, L.; Merbach, A. *Science* **2001**, *291*, 856–859.
25. Akesson, R.; Pettersson, L. G. M.; Sandstrom, M.; Wahlgren, U. *J. Phys. Chem.* **1992**, *96*, 150–156.
26. Jahn, H.; Teller, E. *Proc. R. Soc. London, Ser. A* **1937**, *161*, 220–225.
27. Ferro, D. R.; Provasoli, A.; Ragazzi, M.; Casu, B.; Torri, G.; Bossennec, V.; Perly, B.; Sinay, P.; Petitou, M.; Choay, J. *Carbohydr. Res.* **1990**, *195*, 157–167.
28. Ferro, D. R.; Provasoli, A.; Ragazzi, M.; Torri, G.; Casu, B.; Gatti, G.; Jacquinet, J. C.; Sinay, P.; Petitou, M.; Choay, J. *J. Am. Chem. Soc.* **1986**, *108*, 6773–6778.
29. Noda, I. *Appl. Spectrosc.* **1990**, *44*, 550–561.
30. Noda, I. *Appl. Spectrosc.* **1993**, *47*, 1329–1336.
31. Stevens, E. S.; Morris, E. R.; Rees, D. A.; Sutherland, J. C. *J. Am. Chem. Soc.* **1985**, *107*, 2982–2983.
32. Braud, C.; Vert, M. *Macromolecules* **1985**, *18*, 856–862.
33. Yates, E. A.; Santini, F.; Guerrini, M.; Naggi, A.; Torri, G.; Casu, B. *Carbohydr. Res.* **1996**, *294*, 15–27.
34. Mabbs, F. E.; Collison, D. *Electron Paramagnetic Resonance of d-Resonance Metal Compounds. Studies in Inorganic Chemistry*; Elsevier: Amsterdam, 1992.
35. Patey, S. J.; Edwards, E. A.; Yates, E. A.; Turnbull, J. E. *J. Med. Chem.* **2006**, *49*, 6129–6132.
36. Skidmore, M. A.; Guimond, S. E.; Dumax-Vorzet, A. F.; Atrih, A.; Yates, E. A.; Turnbull, J. E. *J. Chromatogr. A* **2006**, *1135*, 52–56.